New Unifying Concepts for Modeling Smart Materials

William S. Oates

Florida Center for Advanced Aero-Propulsion–FCAAP
Department of Mechanical Engineering
Florida A&M/Florida State University
Tallahassee, FL 32310-6046

ABSTRACT

Material modeling techniques for active materials include a broad number of approaches that are often focused on predicting a specific field-coupled constitutive relation. This field-coupled material behavior may include electro-mechanical, magnetostrictive, thermal or light induced phase transformations, or ionic deformation. Limited work has been conducted on developing a unified theory. Such theories are useful for quantifying underlying field-coupled mechanics concepts that may otherwise be neglected in phenomenological models. The theoretical approach presented here employs nonlinear continuum mechanics coupled to a set of microscale order parameters that describe microstructure evolution and phase changes. Unifying concepts are obtained which illustrate how material constants such as piezoelectric coefficients depend on the choice of the order parameter and mechanical energy function without introducing explicit phenomenological coupling parameters.

Keywords: nonlinear continuum, unified model, ferroic materials, functional elastomers

1. INTRODUCTION

A considerable amount of modeling research has been conducted on active materials to understand the field-coupled constitutive behavior. These materials are applicable to areas including information technology, robotics, aerospace systems, automotive components, and biomedical devices. Models ranges from continuum, micromechanics, phase field, atomistic, and *ab initio* have contributed to important relations governing this class of materials. One notable example of an unified material model for ferroic materials is the homogenized energy approach which has been applied to 1D loading and some limited multiaxial loading cases.[1–3] Other examples that describe electro-magneto-mechanics in a unified manner are described in,[4–6] but these analyses focus primarily on the balance laws with limited examples of specific thermodynamic energy functions and comparisons with data.

Active materials cover a broad class of single crystals, ceramics, metals, and polymers which are classified by a shape change in response to an external stimuli such as electric or magnetic fields, heat, light, or chemical absorption. Conversely, many of these materials change their internal state in response to deformation which provides sensing capabilities. Some of the most well-known compositions include ferroelectrc materials, magnetostrictive compounds, and shape memory alloys.[7–9] Soft or glassy elastomer materials and nanocomposites have also drawn attention recently.[10–12]

To address the growing challenge of understanding the vast array of active material responses, a nonlinear continuum model and thermodynamic energy function are presented that couple different microscale internal state order parameters with mechanics. This provides a methodology that is based solely on nonlinear geometric effects coupled to microstructure evolution. Piezoelectric coefficients, for example, are obtained without explicitly introducing these coefficients within the energy description. A similar approach has been considered for quantifying "Maxwell" stresses in soft dielectric materials.[13,14] In the dielectric elastomer example, implementation of an invariant form of the free energy in the reference description leads to stresses that are equivalent to Maxwell's stress if the dielectric energy is an ideal quadratic function of polarization. Another example is a liquid crystal elastomer which is described by an internal director that defines the local orientation of the

Further author information: E-mail: woates@eng.fsu.edu, Telephone: 1 (850)410-6190

liquid crystal mesogens (i.e., liquid crystal forming molecule). These molecules are attached to the polymer network which can produce unusual deformation.[15] Unlike quadratic potentials that are used to define linear dielectric behavior, the energy function that describes liquid crystal behavior is non-convex. This can give anisotropic deformation and soft elastic responses as the liquid crystals rotate or evolve from a monodomain into a polydomain state.[16,17]

This modeling approach is extended here to other smart materials with active microstructure. The approach uses the deformation gradient to obtain field-coupled material behavior similar to the approach presented in[14,16] for soft elastomer materials. Alternatively, the rotation tensor could be used to satisfy rotational invariance; however, obtaining the Cauchy stress tensor is more challenging.[13] In this analysis, non-convex energy functions that describe the order parameter that is coupled to the deformation gradient are explored to provide a more general modeling framework for a broad class of active materials. This provides a framework that describes ferroic material behavior and anisotropic deformation as a function of the orientation of the order parameter, but is also more general and can be implemented to quantify effects such as ionic diffusion in polymers, biological materials, or chemically deforming materials. The model also reduces to the conventional Maxwell stress governing dielectric materials if the order parameter energy function is a quadratic potential. Two numerical examples are given to describe the unified properties of the model for different types of active materials. The model is applied to ferroelectric ceramics such as lead zirconate titanate (PZT)[18] and a liquid crystal elastomer that deforms in the presence of water vapor.[19]

The outline of the paper is given as follows. In Section 2, the governing equations are given which include balance laws in the reference description and general energy function relations in both the spatial and reference frames. In Section 3, specific forms of the free energy are introduced and field-coupled stresses are quantified for a vector and scalar order parameter which will be used to describe the crystal structure and phase evolution, respectively. In Section 4, the model is implemented numerically and compared to data in the literature on ferroelectric ceramics and humidity responsive liquid crystal elastomers. Concluding remarks are given in the final section.

2. GOVERNING EQUATIONS

The model is developed by starting with a free energy description in the spatial configuration per current volume

$$\psi = \psi_M(F_{iK}) + \psi_A(\rho, \rho_{,i}, \phi_i, \phi_{i,j}) \tag{1}$$

where ψ_M is the mechanical energy and ψ_A is the "active" energy associated with a vector order parameter $\phi_i = \{P_i, M_i, n_i\}$ which may denote polarization (P_i), magnetization (M_i), or liquid crystal order (n_i), for example. The gradient on the order parameter ($\phi_{i,j}$) is often included in meso to microscale energy descriptions to predict the effect of twinned domain structures within a grain or single crystal material. The scalar order parameter ρ and its gradient $\rho_{,i}$ denote the density and density gradient of the material; respectively. It should be noted that this is not the most general choice for an active material energy function since the mechanical and "active" energy components are assumed to be decoupled. This decoupled form is used to eliminate any potential unnecessary intricacies within the modeling framework.

It is initially assumed that these materials can undergo finite deformation without fracture. The assumption of large deformation is used to quantify the material coupling based on nonlinear geometric effects, but the model is also applicable in the limit of infinitesimal strain. The introduction of finite deformation is found to be useful in obtaining a set of unified coupling relations between the deformation and each order parameter given in (1). Deformation induced by the order parameter in the limit of infinitesimal strain will also be assessed for comparisons with well-known ferroelectric compositions such as lead-zirconate-titanate (PZT).[18]

The nonlinear continuum model uses the deformation gradient

$$F_{iK} = \frac{\partial x_i}{\partial X_K} \tag{2}$$

where x_i is the spatial point and X_K is the reference or material point.[20]

A number of mechanical energy functions can be introduced to quantify stress-strain constitutive behavior such as an anisotropic elastic constitutive law, or in the case of elastomers, a hyperelastic energy function; see[21] for examples. Here, coupling between a generalized mechanical energy function is used to illustrate unifying trends in smart materials. Specific elastic and order parameter energy functions will be given in subsequent sections to provide some quantitative estimates for different active materials.

Coupling between stretching bonds mechanically and the order parameters is illustrated by writing the energy and field relations in the reference configuration. The vector order parameter and its gradient in the reference and current configuration are related by

$$\begin{aligned} \phi_i &= J^{-1}F_{iK}\widetilde{\phi}_K \\ \phi_{i,j} &= J^{-1}F_{iK}F_{jL}\widetilde{\phi}_{K,L} \end{aligned} \tag{3}$$

where $\widetilde{\phi}_K$ and $\widetilde{\phi}_{K,L}$ are the order parameter and order parameter gradient in the reference configuration, respectively. The Jacobian is defined by $J = \det(F_{iK})$. These relations can be obtained using the principle of virtual work by introducing work conjugate variables for the order parameter and its gradient; see[16] for an example on liquid crystal elastomers.

A similar set of relations are obtained from virtual work principles for the density and its gradient. These relations are

$$\begin{aligned} \rho &= J^{-1}\widetilde{\rho} \\ \rho_{,i} &= J^{-1}F_{iK}\widetilde{\rho}_{,K} \end{aligned} \tag{4}$$

where the density order parameter and its gradient in the reference configuration are denoted by $\widetilde{\rho}$ and $\widetilde{\rho}_{,K}$, respectively.

These field relations are implemented to quantify the energy in the reference domain. The free energy is defined to be equivalent in both the reference and spatial domain according to

$$\Psi = \int_{\Omega} \psi dV = \int_{\Omega_0} \psi J dV_0 = \int_{\Omega_0} \widetilde{\psi} dV_0 \tag{5}$$

where dV is the current volume element over the domain Ω in the current configuration and dV_0 is the reference volume element over the domain Ω_0 in the reference configuration. The relation $dV = JdV_0 = \det(F_{iK})dV_0$ has also been used. These relations provide the transformation

$$\widetilde{\psi} = J\psi. \tag{6}$$

Based on the above relations, the free energy density of the order parameter in the reference domain is governed by

$$\widetilde{\psi}_A = \widetilde{\psi}_A(F_{iK}, \widetilde{\rho}, \widetilde{\rho}_{,K}, \widetilde{\phi}_K, \widetilde{\phi}_{K,L}) \tag{7}$$

per reference volume. This illustrates coupling between the deformation gradient and the order parameter without introducing explicit coupling parameters.

Minimization of the total free energy $\widetilde{\psi} = \widetilde{\psi}_M + \widetilde{\psi}_A$ per reference volume requires satisfying linear momentum and microscale force balances on the order parameters $\widetilde{\phi}_K$ and $\widetilde{\rho}$. These equations are

$$\begin{aligned} \frac{\partial s_{iK}}{\partial X_K} &= 0 \\ \frac{\partial \widetilde{\xi}_{JI}}{\partial X_J} + \widetilde{\pi}_I + \widetilde{\gamma}_I &= 0 \\ \frac{\partial \widetilde{\xi}_I}{\partial X_I} + \widetilde{\pi} + \widetilde{\gamma} &= 0 \end{aligned} \tag{8}$$

in the reference frame where the first equation is linear momentum, the second equation describes a microforce balance on the order parameter $\widetilde{\phi}_I$, and the last equation is an additional microforce balance on the density $\widetilde{\rho}$; see[22] for a similar approach. The nominal stress is defined by s_{iK} and the body forces and inertial forces are neglected. The microforce balance is governed by the micro-stress tensor $\widetilde{\xi}_{JI}$, an internal body force $\widetilde{\pi}_I$, and an external body force $\widetilde{\gamma}_I$. An analogous set of work conjugate variables are defined for the phase where $\widetilde{\xi}_I$ is a interface tension, and $\widetilde{\pi}$ and $\widetilde{\gamma}$ are intrinsic and extrinsic chemical potentials; respectively.

The relation given by $(8)_3$ is normally coupled to conservation of mass and a phenomenological diffusion relation in terms of a chemical potential gradient.[22] The coupling between conservation of mass and the microforce chemical balance leads to the classic Cahn-Hilliard equation.[23] Details of this derivation in the reference configuration is not given here. Instead, material behavior at equilibrium is considered while excluding density gradient penalties in the energy function. This results in $\widetilde{\xi}_I = 0$. The chemical potential will then be defined by the relation $\widetilde{\mu} = \dfrac{\partial \widetilde{\psi}}{\partial \widetilde{\rho}}$. This definition can then be related to the potential $\widetilde{\pi}$.[22] Note that this also requires that the extrinsic potential $\widetilde{\gamma}$ to be zero.

In addition to the work conjugate relation for the chemical potential, the thermodynamic relations for the vector order parameter are defined. Here, the extrinsic microforce $\widetilde{\gamma}_I$ is set to zero and the internal microforce is $\widetilde{\pi}_I = -\widetilde{\eta}_I - \beta_{IJ}\dot{\widetilde{\phi}}_J$ where the second term is a rate dependent dissipative microforce. The conservative microforce and microstress conjugate variables are

$$\widetilde{\eta}_I = \frac{\partial \widetilde{\psi}}{\partial \widetilde{\phi}_I} \quad \text{and} \quad \widetilde{\xi}_{JI} = \frac{\partial \widetilde{\psi}}{\partial \widetilde{\phi}_{I,J}} \tag{9}$$

where the first term is the microforce and the second term is the microstress.

Coupling between the mechanical response of the material and the order parameter is illustrated using the definition of the nominal stress.[21] Recall that that free energy in the reference domain is defined by $\widetilde{\psi} = \widetilde{\psi}_M + \widetilde{\psi}_A$ which gives the nominal stress

$$s_{iK} = \frac{\partial \widetilde{\psi}_M}{\partial F_{iK}} + \frac{\partial \widetilde{\psi}_A}{\partial F_{iK}} \tag{10}$$

where the first term is stress from mechanically stretching the bonds within the material and the second term is internal stress induced by each order parameter and possibly higher order gradients. This illustrates how an order parameter (e.g., polarization, magnetization, liquid crystal order, or phase) influences the constitutive behavior of an active material. It demonstrates how the field-coupled stress, $s^A_{iK} = \dfrac{\partial \widetilde{\psi}_A}{\partial F_{iK}}$ will influence the deformation of the material. In addition, changes in the deformation will influence reorientation of the order parameter. These effects are illustrated through numerical examples in the following section.

3. FREE ENERGY DESCRIPTION

First, a description of energy relations governing a vector order parameter are given followed by an energy function that governs deformation from absorption of chemical constituents from the environment. The vector order parameter is used to describe materials with active microstructure such as ferroelectric materials, magnetostrictive compounds, shape memory alloys, and liquid crystal elastomers. The energy function describing absorption behavior constitutes a chemical free energy and will be used here to describe water vapor absorption into a specific liquid crystal elastomer.[19] The result is general and can be extended to other chemical absorption coupling with deformation.

3.1 Vector Order Parameter

The thermodynamic energy function that is used to predict crystal structure evolution and coupling to deformation is divided into two components. The first component describes crystal anisotropy. This function is well-known for describing the easy axis of ferromagnetic materials but applicable to other materials include ferroelectric compositions and shape memory alloys.[8,24,25] This potential function gives low energy states along certain crystallographic orientations. The second energy function is non-convex near the origin and is used to describe the magnitude of the vector order parameter at equilibrium. This energy is often used to describe liquid crystals since many of these materials have a rod shape at the molecular scale, but no long range interaction (excluding smectic phases).[15,26] The superposition of these two energy functions are often sufficient to describe many ferroic materials.[25]

The first thermodynamic potential defines crystal anisotropy in terms of the order parameter

$$\psi_\phi = \frac{b_{ijkl}}{4}\phi_i\phi_j\phi_k\phi_l \tag{11}$$

where the phenomenological parameters b_{ijkl} are written as a fourth order tensor that defines crystal anisotropy. This fourth order potential gives a set of crystal orientations with low energy states. This tensor can often be reduced to a small number of material parameters using symmetry arguments. A numerical example for tetragonal phase ferroelectric materials will be given using a scalar parameter for b_{ijkl}. See Figure 1(a) for a plot of this function for tetragonal phase materials.

The potential defined by (11) constrains the order parameter along certain crystal crystallographic orientations; however, it does not constrain the order parameter to a fixed magnitude. This requires an additional energy function that penalizes large order parameter magnitudes

$$\psi_Q = cQ_{ii} + \frac{d}{2}Q_{ij}Q_{ij} \tag{12}$$

where two additional phenomenological parameters, c and d, have been introduced. The second order tensor Q_{ij} is

$$Q_{ij} = \frac{1}{2}(3\phi_i\phi_j - \delta_{ij}) \tag{13}$$

which defines a traceless tensor often used to model liquid crystals.[26] This tensor includes deviatoric properties of the order parameter ϕ_i by subtracting the hydrostatic component, i.e., $\mathrm{Tr}(\boldsymbol{\phi}\cdot\boldsymbol{\phi})$. Also note that this second order tensor assumes the vector order parameter has been normalized at its equilibrium state. This energy function is plotted in Figure 1(b).

The second order tensor is related to the work conjugate variable η_i using the relation

$$\eta_i = \frac{\partial\psi}{\partial Q_{kl}}\frac{\partial Q_{kl}}{\partial\phi_i} \tag{14}$$

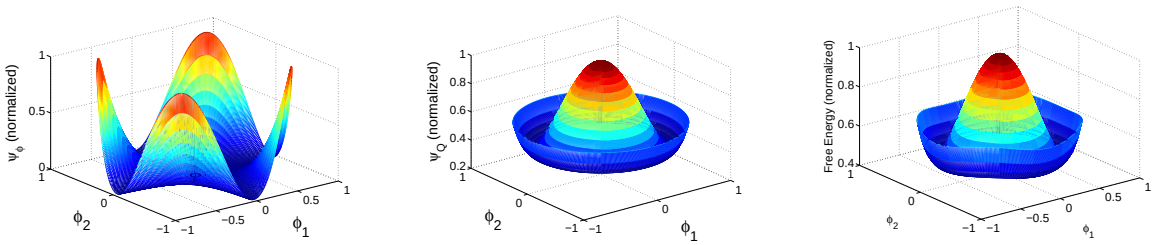

(a) (b) (c)

Figure 1: Free energy plots for the unified model. (a) Anisotropy energy described by ψ_ϕ in (11). (b) Energy described by ψ_Q in (12). (c) The total Landau energy $\psi = \psi_\phi + \psi_Q$.

In addition, virtual work principles are used to relate the second order tensor Q_{ij} to the reference frame. This is achieved using

$$Q_{ij} = J^{-1} F_{iK} F_{jL} \widetilde{Q}_{KL} \tag{15}$$

as described in Oates and Wang.[16]

It should be noted that the energy defined by ψ_Q provides no driving force towards a specific crystallographic orientation, but constrains the order parameter to a finite value along any orientation. For ferroic materials with long range order, the combined effect using, $\psi_A = \psi_\phi + \psi_Q$, gives a set of energy minima along specific crystallographic directions. The sum of these energy components for two dimensional problems is plotted in Figure 1(c). The parameters used in this energy are given in Table 1. Small values are used for the parameters in b_{ijkl} as motivated by fits to piezoelectric lead zirconate titanate. This is discussed in Section 4.1.

The energy function ψ_A has been defined in the spatial domain per current volume. A transformation to the reference domain is introduced to numerically implement the model in the reference configuration. This transformation is obtained by substitution of $(3)_1$ and (6) into (11). This gives a free energy of the form

$$\widetilde{\psi}_\phi = \frac{\widetilde{b}_{KLMN}}{4} \widetilde{\phi}_K \widetilde{\phi}_L \widetilde{\phi}_M \widetilde{\phi}_N \tag{16}$$

where the following parameter has been defined

$$\widetilde{b}_{KLMN} = J^{-3} F_{iK} F_{jL} F_{pM} F_{qN} b_{ijpq} \tag{17}$$

Similarly, substitution of (6) and (15) into (12)

$$\psi_Q = c_{KL} \widetilde{Q}_{KL} + \frac{d_{IJKL}}{2} \widetilde{Q}_{IJ} \widetilde{Q}_{KL} \tag{18}$$

where the following parameters have been defined

$$\begin{aligned} c_{KL} &= F_{iK} F_{iL} c \\ d_{IJKL} &= J^{-1} F_{iK} F_{jL} F_{iM} F_{jN} d. \end{aligned} \tag{19}$$

The nominal stress induced by the order parameter is obtained through the relation,

$$s^A_{iK} = \frac{\partial \widetilde{\psi}_A}{\partial F_{iK}} \tag{20}$$

which gives

$$\begin{aligned} s^{\phi}_{rS} &= b_{rjmt} J^{-3} F_{jL} F_{mP} F_{tQ} \widetilde{\phi}_S \widetilde{\phi}_L \widetilde{\phi}_P \widetilde{\phi}_Q \cdots \\ &\quad -\frac{3 b_{ijmt}}{4} J^{-3} H_{rS} F_{iK} F_{jL} F_{mP} F_{tQ} \widetilde{\phi}_K \widetilde{\phi}_L \widetilde{\phi}_P \widetilde{\phi}_Q \end{aligned} \tag{21}$$

based on (16) and

$$\begin{aligned} s^{Q}_{rS} &= 2c F_{rM} Q_{SM} + 2d J^{-1} F_{jK} F_{rM} F_{jN} \widetilde{Q}_{KS} \widetilde{Q}_{MN} \cdots \\ &\quad -\frac{d}{2} J^{-1} H_{rS} F_{iK} F_{jL} F_{iM} F_{jN} \widetilde{Q}_{KL} \widetilde{Q}_{MN} \end{aligned} \tag{22}$$

based on (18) where the relation $\dfrac{\partial J}{\partial F_{iK}} = J H_{iK}$ has been applied; see Holzapfel[21] for details. The inverse deformation gradient H_{iK} has been introduced which is defined by $H_{iK} F_{jK} = \delta_{ij}$. The total order parameter coupled nominal stress is defined by $s^A_{rS} = s^{\phi}_{rS} + s^Q_{rS}$.

The Cauchy stress induced by the order parameter is obtained from the nominal stress using the relation

$$\sigma^A_{ij} = J^{-1} F_{jK} \frac{\partial \widetilde{\psi}_A}{\partial F_{iK}}. \tag{23}$$

see[20] for details.

A substitution of the energy function for ψ_A into (23) gives a more compact form of the field-coupled stress

$$\sigma^A_{ij} = b_{istq} \phi_s \phi_t \phi_q \phi_j - \frac{3}{4} b_{rstq} \phi_r \phi_s \phi_t \phi_q \delta_{ij} + 2c Q_{ij} + 2d Q_{ik} Q_{jk} - \frac{d}{2} Q_{mn} Q_{mn} \delta_{ij}. \tag{24}$$

This Cauchy stress illustrates the coupling due to nonlinear geometric effects associated with the order parameter ϕ_i and higher order tensor Q_{ij}. It should be noted that this is not the only form of a non-convex energy function that may be used to represent crystal anisotropy. The form used here was chosen to partially decouple short range order in (ψ_Q) and crystal anisotropy effects in (ψ_ϕ). It has also neglected higher order gradients which may be necessary to quantify twinned microstructures that contain interface energy. These effects on stress can be obtained in a similar manner.

It should be noted that the stress in (24) will be balanced with mechanical forces induced by the mechanical energy. In the case of zero traction boundary conditions, the *total* stress is zero. The total stress is defined as the sum of the mechanically induced stress from stretching bonds within the material and the stress from the order parameters. For this case, the spontaneous strain can be obtained as a function of the Landau coefficients and elastic or hyperelastic material parameters. The modulus and Landau parameters provide an inverse relationship for spontaneous strain, i.e., smaller spontaneous strain occurs as the modulus increases.

The Cauchy stress in (24) describes the converse field-coupled effect. The direct effect or sensing response is described by the microforce and microstresses in the reference configuration. These work conjugate variables are

$$\begin{aligned} \widetilde{\eta}_I &= \frac{\partial \psi}{\partial \widetilde{\phi}_I} \\ \widetilde{\xi}_{JI} &= \frac{\partial \psi}{\partial \widetilde{\phi}_{I,J}} \end{aligned} \tag{25}$$

and by implementing the energy functions (16) and (18) with parameters in (17) and (19), obvious coupling with deformation is obtained. As an example, consider a ferroelectric. The microforce $\widetilde{\eta}_I$ would be related to an electric field induced by the polarization, $\widetilde{P}_I = \widetilde{\phi}_I$. Additional microstresses may occur along domain walls where $\widetilde{P}_{I,J} \neq 0$.

3.2 Scalar Order Parameter

A chemical free energy per current volume is introduced using the relation

$$\psi_\rho(\rho) = \frac{g}{2}(\rho - \rho_0)^2 + \frac{h}{4}(\rho - \rho_0)^4 \tag{26}$$

where the nominal density of the material is ρ_0. The phenomenological parameters include g and h which define the magnitude of the chemical potential. The magnitudes of these parameters give a double well potential if $g < 0$ and $h > 0$. This is often used to describe spinodal decomposition as discussed by Lupis.[27] The model will be later restricted to a quadratic potential (i.e., $g > 0$ and $h = 0$) to describe a linear driving force for absorption of relative humidity within a liquid crystal elastomer. The generalized form of the stress induced by changes in the density is given as follows.

Nonlinear coupling between the deformation gradient and the phase is introduced within this energy function using the relation previously defined by $(4)_1$. This requires that the free energy in the reference frame be coupled to the deformation gradient via the Jacobian J as described by

$$\widetilde{\psi}_\rho = \frac{g}{2}J^{-1}(\widetilde{\rho} - \rho_0)^2 + \frac{h}{4}J^{-3}(\widetilde{\rho} - \rho_0)^4. \tag{27}$$

The stress associated with the change in concentration is obtained from $s^\rho_{iK} = \dfrac{\partial \widetilde{\psi}_\rho}{\partial F_{iK}}$ which gives

$$s^\rho_{iK} = -\frac{g}{2}J^{-1}H_{iK}(\widetilde{\rho} - \rho_0)^2 - \frac{3h}{4}J^{-3}H_{iK}(\widetilde{\rho} - \rho_0)^4 \tag{28}$$

and the Cauchy stress is obtained using the relations (4), (23), and (28)

$$\sigma^\rho_{ij} = -\left(\frac{g}{2}(\rho - \rho_0)^2 + \frac{3h}{4}(\rho - \rho_0)^4\right)\delta_{ij}. \tag{29}$$

This stress will be implemented in the following section to show bending deformation in a liquid crystal elastomer that is exposed to water vapor on one side.

4. NUMERICAL IMPLEMENTATION

Two examples are given to describe how this model can be used to predict deformation as a function of the evolution of the underlying microstructure or phase change. First an example is given for a ferroelectric material and compared to data given by Jones et al.[28] Second, deformation of a liquid crystal elastomer in the presence of water vapor are modeled and compared to experiments given by Harris et al.[19]

4.1 Ferroelectric Material Model

A ferroelectric Landau thermodynamic potential is introduced in combination with an isotropic elastic energy. Piezoelectric coupling is quantified as a function of the Landau and elasticity coefficients for different polarization orientations. It is found that the result qualitatively matches anisotropic piezoelectric behavior as a function of polarization orientation as described in Jones et al.[28]

Crystal anisotropy as a function of the polarization is obtained by combining the energy functions previously given by (11) and (12) and illustrated in Figure 1. The vector order parameter is defined by $P_i = \phi_i$ in the spatial frame and $\widetilde{P}_I = \widetilde{\phi}_I$ in the reference frame. Tetragonal phase ferroelectric materials are considered which requires the following non-zero b_{ijkl} components: $b_{1122} = b_{2211} = b_{1133} = b_{3311} = b_{2233} = b_{3322}$. The Landau parameters, Young's modulus, and Poisson ratio used in the model are given in Table 1. These parameters were previously used in the energy plots given in Figure 1.

The polarization induced deformation at equilibrium under varying electric fields is determined by minimizing the Landau energy $\widetilde{\psi}$ at each field load step under zero stress conditions. These results were obtained by formulating the model in the reference domain and minimizing the energy per reference volume ($\widetilde{\psi}_A$) at each electric field load step using a gradient based approach. The stress was assumed to be zero everywhere in the volume. The deformation gradient was included in the model to ensure accurate prediction of spontaneous strain and coupling to changes in polarization under applied electric fields. Using the parameters in Table 1, the spontaneous strain was $\varepsilon^s_{33} = 0.162\%$, $\varepsilon^s_{22} = \varepsilon^s_{11} = -0.158\%$ for a ferroelectric with polarization oriented in the X_3 direction. The spontaneous polarization for this case is $P^s_3 = 0.66$ C/m^2. Refined model predictions can be achieved with higher order expansions on the Landau energy function.

The polarization order parameter is rotated in the $X_2 - X_3$ plane to quantify changes in the piezoelectric response as a function of polarization orientation. It is found that this has a dramatic effect on the piezoelectric response. The piezoelectric response for different crystal orientations is illustrated in Figure 2. The piezoelectric coefficient d_{333} is found to be slightly negative when aligned with the field ($\theta = 90^o$). As the angle is reduced, the coefficient d_{333} increases until it reaches a maximum near $\theta = 54^o$ and then approaches zero as the angle approaches zero. It should be noted that this is an idealized case of a single crystal. In poled ceramics or polydomain single crystals, a negative d_{333} at $\theta = 90^o$ is unlikely due to inhomogeneities in the orientation of the polarization which more closely correlates with data in Jones et al.[28]

4.2 Diffusion Deforming Materials: Water Vapor Absorption Example

The example of deformation induced by water vapor absorption is motivated by recent experiments presented by Harris et al.[19] on a liquid crystal elastomer. These materials deform in the presence of water or pH differences due to a change in the liquid crystalline structure as the chemical constituents are absorbed within the material and disrupt molecular order. The liquid crystal elastomer structure initially consist of both covalent and secondary bonds. Humidity-controlled motion occurs after the network is convert to a salt. This provides a hygroscopic material which begins to swell under humid conditions as water infiltrates the material and interacts with the liquid crystals that are attached to the elastomer network.

Table 1: Ferroelectric material parameters where b_{1122}, c, and d are Landau parameters and E and ν are the Young's modulus and Poisson ratio, respectively.

b_{1122}	$2.25 \times 10^{-4}\ \frac{\text{N-m}^6}{\text{C}^4}$
c	$-1.875 \times 10^{-4}\ \frac{\text{N-m}^2}{\text{C}^2}$
d	$1.200 \times 10^{-4}\ \frac{\text{N-m}^6}{\text{C}^4}$
E	80 GPa
ν	0.3

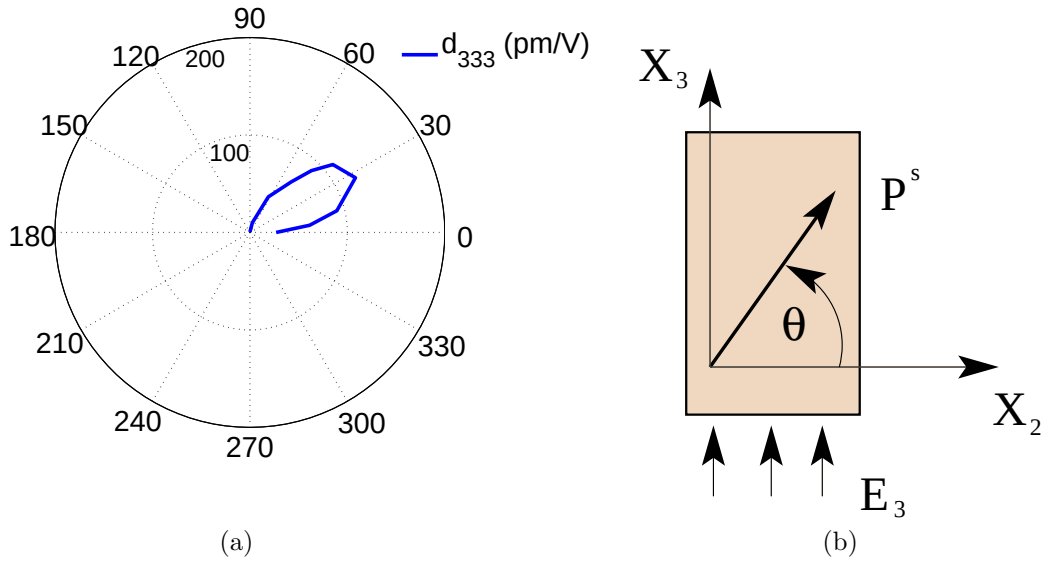

(a) (b)

Figure 2: Polar plot of the piezoelectric coefficient d_{333} as a function of the polarization orientation. The model is rotated in the $X_2 - X_3$ plane. The maximum value is $d_{333} = 420$ pm/V at $\theta = 54^o$ based on the parameters in Table 1.

Prediction of this deformation is obtained by implementing the stress coupling described in Section 3.2 into the linear momentum balance equation. Linear momentum is coupled to a diffusion equation to predict deformation as water vapor absorbs into the material. A cantilever beam is used to describe the deformation and is solved using the finite element method. A commercial package, Comsol, is used to solve the governing equations. The two coupled governing equations are

$$\begin{aligned} &\int_{\Omega_0} \frac{\partial w_i}{\partial X_K} s_{iK} dV_0 = \int_{\Gamma_0} s_{iK} \hat{N}_K w_i dS_0 \\ &- \int_{\Omega_0} D \frac{\partial w}{\partial X_K} \frac{\partial \widetilde{\mu}}{\partial X_K} dV_0 + \int_{\Gamma_0} D \widetilde{\mu}_{,K} \hat{N}_K w dS_0 = \int_{\Omega_0} w \frac{\partial \widetilde{\rho}}{\partial t} dV_0 \end{aligned} \tag{30}$$

where the first equation is linear momentum and w_i is the weight function. The nominal stress is defined by $s_{iK} = s^M_{iK} + s^\rho_{iK}$ where s^ρ_{iK} was previously defined by (28) and s^M_{iK} is a mechanical stress defined by a neo-Hookean hyperelastic energy function.[21] Body forces and inertial effects are neglected. The unit normal in the reference frame is denoted by $\hat{N}_K$. The second equation describes the diffusion of water vapor into the elastomer film where w is the weight function and D is the diffusion coefficient. Also recall that the chemical potential of the water vapor that is absorbed into the solid is $\widetilde{\mu} = \dfrac{\partial \widetilde{\psi}}{\partial \widetilde{\rho}}$.

A cantilever beam is modeled using the parameters defined in Table 2. The boundary conditions and nonlinear finite element solution are illustrated in Figure 3. It is assumed that relative humidity creates a 1% change of density on the surface. The nominal density of the elastomer was assumed to be ρ_0 =1000 kg/m^3. This boundary condition creates diffusion into the material and bending away from the relative humidity source. Bending occurs as the density increases on the top surface similar to experimental results given in Harris et al.[19] The cantilever is 1 mm long and gives a displacement of 1×10^{-6} μm at the tip. Whereas this appears small, the displacement scales with the length of the film as $\sim l^3$ to l^4 based on beam theory. Therefore bending on the order of millimeters occurs for films with length on the order of centimeters which is similar to experimental results.

Table 2: Water vapor deforming material properties. The shear modulus and bulk modulus are denoted by μ_M and κ, respectively.

g	2×10^9 N-mm^4/kg^2
h	0
D	1×10^{-5} kg-s/m^3
μ_M	370 MPa
κ	1.1 GPa

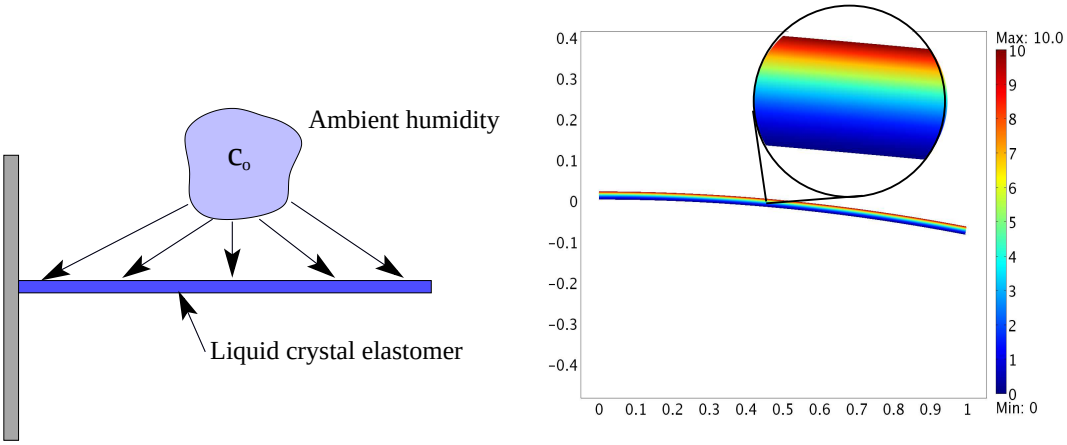

(a) (b)

Figure 3: Schematic and finite element result of a water vapor controlled liquid crystal elastomer. The color field represents the change in density ($\widetilde{\rho} - \rho_0$ in units of kg/m^3) associated with the amount of water vapor absorbed on the top surface.

5. CONCLUDING REMARKS

A nonlinear continuum model is developed by introducing microstructure and phase evolution within the thermodynamic framework. Coupling between the order parameters and finite deformation is established using virtual work principles to illustrate natural coupling between active material microstructure and deformation. Further, deformation will create changes in the local order parameter which governs sensing behavior. An interesting result presented here is prediction of anisotropic piezoelectric coupling in ferroelectric materials. Prior models have assumed that the tetragonal lattice structure extends from fields aligned with the spontaneous polarization. The model presented here predicts the *opposite*–slight contraction from fields applied in the direction of polarization. As the field rotates relative to the polarization, positive increments in the field give rise to positive deformation in the applied field direction. The results compare surprisingly well with recent x-ray experiments on tetragonal phase PZT Jones et al.[28]

The modeling framework is also extended to materials that undergo phase evolution from chemical absorption. This illustrates the utility of the model to a relatively broad class of active materials. Current work is focused on homogenization and twinned domain structure effects to obtain more quantitative predictions with experiments on a range of active materials.

ACKNOWLEDGMENTS

The author sincerely appreciates many enlightening conversations with Dr. Robert Sierakowski (retired Chief Scientists–Eglin AFRL) during a 2009 summer ASEE faculty program at Eglin AFRL. This material is based upon work supported by the Florida Center for Advanced Aero Propulsion (FCAAP). Any opinions, findings,

and conclusions or recommendations expressed in this publication are those of the author and do not necessarily reflect the views of FCAAP.

REFERENCES

[1] Smith, R., Seelecke, S., Dapino, M., and Ounaies, Z., "A unified framework for modeling hysteresis in ferroic materials," *J. Mech. Phys. Solids* **54**(1), 46–85 (2006).
[2] W. Oates and R. Smith, "Multi-axial homogenized energy model for ferroelectric materials," *Proc. ASME IMECE 2006, Chicago, IL* .
[3] Oates, W., "Multiscale constitutive model development and finite element implementation for magnetostrictive materials," *Proc. ASME IMECE 2007, Seattle, WA* .
[4] Maugin, G., [*Continuum mechanics of electromagnetic solids*], North Holland, Amsterdam (1988).
[5] Ericksen, J., "Magnetizable and polarizable elastic materials," *Math Mech Solids, accepted* (2009).
[6] Vu, D. and Steinmann, P., "Material and spatial motion problems in nonlinear electro- and magneto-elastostatics," *Math Mech Solids, accepted* (2009).
[7] Lines, M. and Glass, A., [*Principles and Applications of Ferroelectrics and Related Materials*], Clarendon Press, Oxford (1977).
[8] Bertotti, G., [*Hysteresis in Magnetism: for Physicists, Materials Scientists, and Engineers*], Academic Press, San Diego, CA (1998).
[9] Boyd, J. and Lagoudas, D., "A thermodynamical constitutive model for shape memory materials. Part II. The sma composite material," *Int. J. Plasticity* **12**(7), 843–873 (1996).
[10] Koerner, H., White, T., Tabirya, N., Bunning, T., and Vaia, R., "Photogenerating work from polymers," *Materials Today* **11**(7–8), 34–42 (2008).
[11] Gall, K., Dunn, M., Liu, Y., Stefanic, G., and Balzar, D., "Internal stress storage in shape memory polymer nanocomposites," *Appl. Phys. Lett.* **85**(2), 290–292 (2004).
[12] Kofod, G. and Sommer-Larsen, P., "Silicone dielectric elastomer actuators: Finite-elasticity model of actuation," *Sensors and Actuators A* **122**, 273–283 (2005).
[13] McMeeking, R. and Landis, C., "Electrostatic forces and stored energy for deformable dielectric materials," *J. Appl. Mech* **72**, 581–590 (2005).
[14] Zhao, X., Hong, W., and Suo, Z., "Electromechanical hysteresis and coexistent states in dielectric elastomers," *Phys. Rev. B* **76**, 134113–1–134113–9 (2007).
[15] Warner, M. and Terentjev, E., [*Liquid Crystal Elastomers–Revised Edition*], Oxford Science Publications, Oxford (2007).
[16] Oates, W. and Wang, H., "A new approach to modeling liquid crystal elastomers using phase field methods," *Modelling Simul. Mater. Sci. Eng.* **17**, 064004 (2009).
[17] Conti, S., DeSimone, A., and Dolzmann, G., "Soft elastic response of stretched sheets of nematic elastomers: a numerical study," *J. Mech. Phys. Solids* **50**, 1431–1451 (2002).
[18] Jaffe, B., Cook, W., and Jaffe, H., [*Piezoelectric Ceramics*], Academic Press, London (1971).
[19] Harris, K., Bastiaansen, C., Lub, J., and Broer, D., "Self-assembled polymer films for controlled agent-driven motion," *Nano Lett.* **5**, 1857–1860 (2005).
[20] Malvern, L., [*Introduction to the Mechanics of a Continuous Medium*], Prentice-Hall, Inc., Englewood Cliffs, NJ (1969).
[21] Holzapfel, G., [*Nonlinear Solid Mechanics*], John Wiley & Sons, Inc., Chichester (2000).
[22] Fried, E. and Gurtin, M., "Generalized ginzburg-landau and cahn-hilliard equations based on a microforce balance," *Physica D* **92**, 178–192 (1996).
[23] J.Cahn, "On spinodal decomposition," *Acta. Metall.* **9**, 795–801 (1961).
[24] Kittel, C., "Physical theory of ferromagnetic domains," *Rev. Mod. Physics* **21**(4), 541–583 (1949).
[25] Smith, R., [*Smart Material Systems: Model Development*], SIAM, Philadelphia, PA (2005).
[26] P. de Gennes and Prost, J., [*The Physics of Liquid Crystals*], Oxford Science Publications, Oxford (1993).
[27] Lupis, C., [*Chemical Thermodynamics of Materials*], Prentice-Hall, New York (1983).
[28] Jones, J., Pramanick, A., Nino, J., Daymond, M., and Oliver, E., "Time-resolved and orientation-dependent electric-field-induced strains in lead zirconate titanate ceramics," *Appl. Phys. Lett.* **90**, 172909 (2007).